Available online at www.sciencedirect.com
ScienceDirect
International Journal of Heat and Mass Transfer 50 (2007) 1344–1355
International Journal of HEAT and MASS TRANSFER
www.elsevier.com/locate/ijhmt

Entropy production for cylinder drying of linerboard and newsprint

G.J.M. Koper [a], S. Kjelstrup [b], T. van de Ven [c], M. Sadeghi [d,*], W.J.M. Douglas [d]

[a] DelftChemTech, Delft University of Technology, Julianalaan 136, 2628 BL Delft, The Netherlands
[b] Department of Chemistry, Norwegian University of Science and Technology, Realfagbygget, D3, No-7491 Trondheim, Norway
[c] Pulp and Paper Research Centre, Department of Chemistry, McGill University, Montreal, QC, Canada
[d] Pulp and Paper Research Centre, Department of Chemical Engineering, McGill University, 3420 University Street, Montreal, QC, Canada H3A 2A7

Received 2 November 2005; received in revised form 15 September 2006
Available online 28 November 2006

Abstract

For industrial paper drying, the entropy production from heat and mass transfer irreversibilities was determined by combining principles of irreversible thermodynamics with information from a dryer simulator. Transport irreversibilities depend on sheet and dryer characteristics. Entropy production for multi-cylinder paper dryer sections was compared for 5 paper machines, producing 3 grades of linerboard, 2 of newsprint. The three major contributions to entropy production were evaluated: entropy production for evaporation of water, for convective heat transfer between the sheet and ambient air, and for cylinder-to-sheet heat conduction. Effects on entropy production from paper basis weight and drying cylinder steam pressure were examined.

Keywords: Paper drying; Entropy production; Irreversible thermodynamics; Drying simulation; Heat transfer; Mass transfer

1. Introduction

Paper production is among the largest energy consuming industries, accounting for about 4% of world energy consumption[1] according to the World Energy Council [1]. The paper machine alone accounts for 35% of the total energy consumption in a pulp and paper mill [2]. On a normalized basis, the energy use is given as the specific energy consumption (SEC), the energy required per tonne of paper. De Beer et al. [2] assessed the possibilities for reducing energy consumption in paper drying and concluded that there is a long term potential for saving in the specific consumption of heat (SEC_h), by up to 90% in the most radical case. Manninen et al. [3] made similar projections. Such a radical change is not realistic as it would require substantial increase in the specific consumption of electric power, the highest grade of energy and the most expensive. However the search for energy reduction by techniques which could be implemented industrially remains a high priority and is the basic motivation for the present study.

Although in the first law of thermodynamics electrical and thermal energy are not differentiated, these two forms give vastly different amounts of work. Replacement of thermal by electrical energy should therefore also be evaluated from a second law perspective where energies can be expressed in terms of the ability to do useful work. Such an analysis can also be used in process optimization where alternative operating conditions are assessed. Thus in order to evaluate new or improved technologies from a perspective of how potential work is used, a second law analysis is needed. In such analyses the lost work (lost exergy) in excess of the minimum work needed to perform the process is calculated. Lost work equals the entropy production in the process times the temperature of the environment.

* Corresponding author. Present address: Department of Chemical and Petroleum Engineering, University of Calgary, 2500 University Drive NW, Calgary, AB, Canada T2N 1N4. Tel.: +1 403 220 5754; fax: +1 403 284 4852.
E-mail address: msadeghi@ucalgary.ca (M. Sadeghi).

[1] Although according to the first law of thermodynamics energy is converted, not consumed, we have used here the standard phrase of "energy consumption" for a process which consumes thermal and electrical energy.

0017-9310/$ - see front matter © 2006 Elsevier Ltd. All rights reserved.
doi:10.1016/j.ijheatmasstransfer.2006.09.006

Nomenclature

B	paper basis weight, dry paper mass per unit sheet area (kg/m^2)
c	moisture content in paper (mol/m^3)
$C_{v,\mathrm{i}}$	specific heat capacity of species i (J/(kg K))
d	paper thickness (m)
$\frac{\mathrm{d}S_{\mathrm{irr}}}{\mathrm{d}t}$	entropy production rate (W/K)
ΔH	vaporization enthalpy of water from paper (J/mol)
$\Delta_{\mathrm{sor}}H$	sorption enthalpy of water to fiber (J/mol)
$\Delta_{\mathrm{vap}}H$	vaporization enthalpy of free water (J/mol)
$H(\mathrm{g})$	enthalpy of water in vapor state (J/mol)
$H(\mathrm{p})$	enthalpy of water in paper (J/mol)
J	molar water flux at paper surface (mol/(m^{2}s))
J'_q	heat flux (J/(m^{2}s))
$J'_{q,\mathrm{a}}$	heat flux between paper surface and ambient (J/(m^{2}s))
$J'_{q,\mathrm{c}}$	heat flux between cylinder surface and paper (J/(m^{2}s))
M	molar mass of water (kg/mol)
p^0	standard pressure (Pa)
p^*	vapor pressure (Pa)
p^*_{p}	vapor pressure in paper (Pa)
R	gas constant (J/(mol K))
t	time (s)
Δt	time lapse of paper in the dryer (s)
T	temperature (K)
u	internal energy density (J/m^3)
w	mass-based moisture content (kg/kg dry paper)
W_{lost}	lost work (J)
X_{a}, X_{v}	thermodynamic forces defined by Eqs. (11) and (12)

Greek symbols

μ_{T}	chemical potential of water at constant temperature (J/mol)
$\mu^{\mathrm{g}}_{\mathrm{T}}$	chemical potential of water at the paper surface at constant temperature (J/mol)
$\mu^{\mathrm{p}}_{\mathrm{T}}$	chemical potential of water in paper at constant temperature (J/mol)
σ_{a}	entropy production rate for heat transfer between the paper surface and ambient air (W/(m^2 K))
σ_{c}	entropy production rate for heat transfer between the cylinder and paper surface (W/(m^2 K))
σ_{s}	entropy production rate defined by Eq. (10) (W/(m^2 K))
σ_{v}	entropy production rate of evaporation (W/(m^2 K))
$\Delta\Sigma_{\mathrm{a}}$	entropy production for heat transfer between the paper surface and ambient (J/(kg K))
$\Delta\Sigma_{\mathrm{c}}$	entropy production for heat transfer between the cylinder and paper surface (J/(kg K))
$\Delta\Sigma_{\mathrm{tot}}$	total entropy production (J/(kg K))
$\Delta\Sigma_{\mathrm{v}}$	entropy production of evaporation (J/(kg K))
Θ	sorption isotherm, Eq. (20)

Subscripts

0	environment
c	cylinder surface
g	gas phase
p	paper
s	dry solids
w	water

Second law analyses are receiving increased attention in the process industries, such as in the production of aluminum [4] and ammonia [5]. Second law efficient design of process units is also growing [6–8]. De Beer et al. [2] reported the exergy losses in a paper machine, but without determining how or where the losses occur. In order to determine the lost work, the entropy production at each stage in the process must be calculated. As no detailed documentation of the entropy production in the process of drying paper has appeared, this is the objective of the present study.

Thus the aim of this investigation is to present such an analysis of paper drying and to consider its relevance for improving the second law efficiency of this process. More specifically, the scope is to determine the local and total entropy production for two major paper products, linerboard and newsprint. Cylinder drying, the standard technology used in the production of printing and heavier grades, is therefore the subject of our first work, thereby establishing a basis for subsequent studies. This objective requires the combination of two elements. The structure of second law analysis must be integrated with performance data, both measured and calculated, for dryer sections of paper machines. The general procedure of determining entropy production, as described by de Groot and Mazur [9], has been used for second law analysis by Nummedal et al. [8] and Johannessen et al. [7]. The measured and calculated performance data for paper dryers are available through the work of Douglas and co-workers for paper drying analysis and simulation [10–15]. To provide estimates for parameters required in the present work but not available from paper machine dryer surveys, the dryer simulator of Sadeghi and Douglas [14,15] was used.

The entropy production rate gives the lost exergy, or dissipated energy, from the Gouy–Stodola theorem [4,6]:

$$\frac{\mathrm{d}W_{\mathrm{lost}}}{\mathrm{d}t} = T_0 \frac{\mathrm{d}S_{\mathrm{irr}}}{\mathrm{d}t} \tag{1}$$

Here T_0 is the temperature of the environment. The entropy production rate can be calculated in two ways, from the difference between the entropy flow into and out of the system, or from the fluxes and their conjugate forces inside the

system. The latter procedure is used here, which enables obtaining information on the sources of the lost exergy. Thus the total entropy production rate for a paper dryer consisting of cylinder dryers is determined from the local values of temperature and local fluxes of water vapor and heat throughout the dryer. The procedure employed here consists of several steps. First the system and its volume elements are defined and the entropy production rate, σ, in a local volume element described. After establishing a consistent set of data, within reasonable limits of uncertainty, the various contributions to the entropy production are calculated for each dryer cylinder as the paper goes from wet to dry. Finally, the results are examined relative to the potential for more energy efficient operation.

2. Conservation of mass and energy

For the determination of entropy production, some of the dryer performance data required derive from measurements in industrial dryers while other values must be obtained from a microscale simulator of a paper dryer. Data coming from either source, actual measurements or predicted by a simulator, are subject to uncertainty. For this reason, prior to calculating the entropy production a short procedure is now presented concerning checking the consistency of the data. With respect to the paper drying simulator, the model used here is the most detailed which has appeared [14] and has been successfully validated against 32 dryer surveys [15] in the most extensive reported validation of a paper drying model. The model has been established to be very reliable in predicting dryer section performance for a great variety of grades of paper, types of dryers and dryer operating conditions, as demonstrated for example by the average error for the uncalibrated prediction of paper machine speed for all 32 tests being only 3%. Another particularly important validation is that the predicted sheet average temperature was within 3 °C of the measurements. This exceptional level of accuracy provides confidence in the simulator predictions.

In addition to the aspect of reliability of the input data, there are two other reasons for the present section. First, the drying model validations have been done mostly for entire dryer sections because that is usually the only data which can be obtained from an industrial dryer. A significant exception is the validation against local paper temperature, as noted above. The entropy production, as presented in the following section, is calculated in increments for each dryer cylinder as the sheet goes from wet to dry. Therefore it is relevant to check the mass and energy balances for each such interval. The second reason is that the paper drying model is based on a microscopic description of transport phenomena inside the sheet during drying, i.e. using sheet thickness direction gradients of moisture, temperature and gas pressure. It has been shown [14] that there can be large differences in these characteristics across the sheet thickness. However, we have not included the contribution of internal transport phenomena to the entropy production. Results of consistency check will demonstrate that provided correct values are used for heat and mass transfer fluxes between the sheet and the cylinder or ambient, the general heat and mass balances will be preserved even if the internal gradients of moisture content and temperature are ignored. In fact, because the surface fluxes of heat and mass transfer reported by the simulator derive from the conditions of temperature and moisture content at the sheet surfaces, which are in turn influenced by the internal distributions of temperature and moisture, the entropy production calculated in the present study reflects the internal resistances to heat and mass transfer. Exact determination of entropy production from internal transport phenomena could be the subject of a future study.

The following relations and symbols are standard in descriptions of mass and energy conservation in process engineering, except for the use of fluxes as defined in non-equilibrium thermodynamics [9]. A volume element of paper at position x in the sheet transport direction is considered. For paper of uniform local moisture content in the thickness direction, the relationship between the mass-based paper moisture content w, in kg/kg dry paper, and the volumetric paper moisture concentration c in mol/m^3 is given by:

$$c = \frac{wB}{Md} \tag{2}$$

where B is the paper basis weight in kg/m^2, d the paper thickness, and M the molar mass of water. Recent studies [13,14] have shown that over some parts of the paper machine during the drying of paper, the local moisture content across the sheet thickness direction can at times range from a very high value, for example 1.7 kg/kg dry paper for a case studied in [14], with the fibers saturated and water in the pores, down to essentially dry paper, e.g. 0.05 kg/kg dry paper. When the moisture content, w, varies substantially, and nonlinearly, in the sheet thickness direction then Eq. (2) yields some average value of the volumetric moisture concentration. As explained earlier, this approximation does not have a direct effect on the entropy production calculation. At the sheet surface the exiting water vapor molar flux J is equal to the loss of water from the element, so:

$$\frac{\mathrm{d}c}{\mathrm{d}t} = -\frac{J}{d} \tag{3}$$

Moisture diffusion in the plane of the sheet need not be included because Hashemi et al. [16] have shown that, on the time scale of the industrial process, lateral moisture transport during paper drying is negligible compared to that in the thickness direction. In terms of the paper moisture content this equation can be written as:

$$\frac{\mathrm{d}w}{\mathrm{d}t} = -\frac{JM}{B} \tag{4}$$

By integrating Eq. (4) the moisture content is obtained as a function of the integrated water flux:

$$w(\Delta t) = w(0) - \frac{M}{B}\int_0^{\Delta t} J\,\mathrm{d}t \tag{5}$$

The upper integration limit is the time from entrance into the dryer taken by a sheet moving at paper machine speed.

Similarly, the energy balance for a volume element of paper is given by:

$$\frac{\mathrm{d}u}{\mathrm{d}t} = -\frac{J'_q + J\Delta H}{d} \tag{6}$$

Here u is the energy density of the paper, J'_q is the net heat flux out of the paper, ΔH is the vaporization enthalpy of water from its state in the paper (p) to water vapor (g). Water is adsorbed more or less strongly in the paper, depending on the moisture content, and this effect is treated. The vaporization enthalpy is therefore:

$$\Delta H = H(\mathrm{g}) - H(\mathrm{p}) = \Delta_{\mathrm{vap}}H + \Delta_{\mathrm{sor}}H(\mathrm{w}) \tag{7}$$

Here $\Delta_{\mathrm{vap}}H$ is the vaporization enthalpy of free water, and $\Delta_{\mathrm{sor}}H(\mathrm{w})$ is the water adsorption enthalpy. At low moisture content, the latter term is important and is a sensitive function of moisture content. With the specific heat capacity at constant volume, C_v in J/(kg K), Eq. (6) leads to:

$$\frac{\mathrm{d}T_\mathrm{p}}{\mathrm{d}t} = -\frac{1}{B(C_{v,\mathrm{s}} + C_{v,\mathrm{w}}w)}(J'_q + J\Delta H) \tag{8}$$

It is assumed that the specific heat capacity of paper is a linear combination from the dry solids, $C_{v,\mathrm{s}}$, and from water $C_{v,\mathrm{w}}$. By rearranging and integrating Eq. (8), the integrated heat flux can be expressed as a function of the sheet thickness direction average values of temperature and moisture content:

$$\frac{1}{B}\int_0^{\Delta t}(J'_q + J\Delta H)\,\mathrm{d}t = C_{v,\mathrm{s}}\{T_\mathrm{p}(\Delta t) - T_\mathrm{p}(0)\} + C_{v,\mathrm{w}}\int_0^{\Delta t} w\frac{\mathrm{d}T_\mathrm{p}}{\mathrm{d}t}\,\mathrm{d}t \tag{9}$$

Eqs. (5) and (9) are used in the analysis of consistency of the mass balance and energy balance, respectively (Section 4.2).

3. Local entropy production

Before presenting the entropy production analysis, it is appropriate to briefly introduce multi-cylinder drying, the universally used system for producing printing and heavier grades of uncoated paper. The dryer section of a paper machine could include from 40 up to 90 cylinders, depending on the thickness of the paper grade in production. A common configuration of cylinders is demonstrated in Fig. 1 where the sheet of paper follows a serpentine patch between the successive cylinders. Synthetic screens, termed dryer fabrics or felts, support the moist, low strength sheet and press it against the cylinders, thereby enhancing the contact heat transfer coefficient and reducing the frequency of sheet breaks. Cylinders are heated by steam from inside. Based on the position of the sheet in dryer section, four phases of drying, identified in Fig. 1, are distinguished:

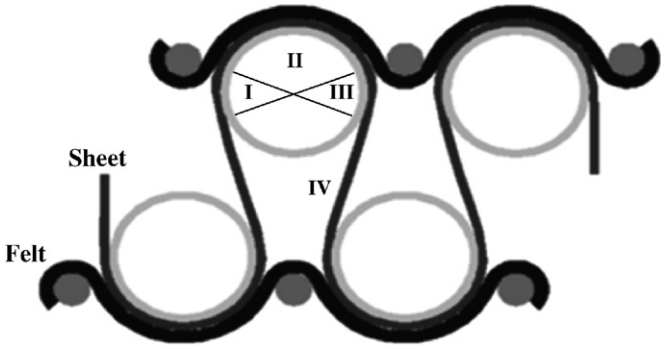

Fig. 1. Serpentine path of paper sheet through a multi-cylinder dryer section. Numbers on the picture refer to the four phases of drying.

Phase I: One side of sheet is in contact with cylinder. Heat is transferred by conduction from the heated cylinder surface to the sheet. Heat and mass transfer (evaporation) occur at the opposite side of the sheet by convection.

Phase II: Sheet is covered by the felt. Heat conduction is active at the cylinder contact side while evaporation and heat transfer occur at the felt surface in touch with ambient air.

Phase III: Felt is removed from the sheet. Transport mechanisms are identical to those of Phase I.

Phase IV: Sheet is passing from one cylinder to the next, with both sides exposed to the ambient air in what is termed the dryer pocket. Evaporation and heat transfer by convection are active on both sides of the sheet.

The drying simulator used in this study takes the presence of the felt into account by incorporating a reduction factor for convective heat and mass transfer coefficients. Therefore the heat and mass transfer fluxes from the sheet, reported by the simulator and used in the entropy production analysis, already include the effect of felt. Consequently, we will need to consider only two general cases:

Case 1: A hot cylinder surface on one side of the sheet and air on the other side.

Case 2: Air on both sides of the sheet, with convective transport of heat and of water vapor between the moist sheet and the adjacent dryer pocket air.

Now the equations are developed for entropy production calculation. The details of the derivation are available elsewhere [17]. For the case of paper drying, the following assumptions are employed:

- Entropy production due to transport phenomena within the sheet is considered negligible.
- Entropy production is considered only due to the heat and mass transfer fluxes between the sheet and the cylinder surface or ambient air.
- Ambient humid air is considered ideal gas.
- Work against the external pressure from volume changes in the paper and from heat flux in the plane of the sheet are neglected.

With the internal entropy production being negligible, we only need to consider the sheet surface temperature, $T(x)$, and the chemical potential of water at this temperature, $\mu_T(x)$. The differences in temperature and chemical potential between the values in the paper and those in the adjacent vapor phase provide the driving forces used in non-equilibrium thermodynamics for the transport of heat and mass, respectively.

Consider first Case 2 above. It was shown by Bedeaux, Kjelstrup and coworkers [17,18] that the entropy production rate per unit area, σ_s, has two terms, one for the mass flux and one for the heat flux between the vapor phase and the phase where there is liquid water. Accordingly, evaporation is accompanied by entropy production:

$$\sigma_s = J'_{q,a}\left(\frac{1}{T_g} - \frac{1}{T_p}\right) - J\frac{1}{T_p}(\mu_T^g - \mu_T^p) \tag{10}$$

The heat flux between the moist paper and the vapor phase is $J'_{q,a}$. Only this flux enters the entropy production rate. The heat flux on the moist paper side of the interface has been eliminated by means of the energy balance [17]. From non-equilibrium thermodynamics the driving force for heat transfer, X_a, defined by the entropy production rate, is the difference in inverse absolute temperatures from the moist paper into the vapor phase:

$$X_a = \frac{1}{T_g} - \frac{1}{T_p} \tag{11}$$

The driving force for mass transfer, likewise defined from the entropy production rate, is the negative of the difference in chemical potential of water from the moist sheet to the water vapor, divided by the absolute temperature of the paper. These chemical potentials are evaluated at the moist sheet temperature and moisture content:

$$X_v = -\frac{1}{T_p}(\mu_T^g - \mu_T^p) \tag{12}$$

The heat and mass fluxes are coupled linearly, i.e. each flux is proportional to each of the forces. It is not necessary to write the flux equations for transfer of heat and mass, as the contributions to σ_s may be calculated directly. Thus the contribution to entropy production from heat transfer is:

$$\sigma_a = J'_{q,a}\left(\frac{1}{T_g} - \frac{1}{T_p}\right) \tag{13}$$

and the entropy production from mass transfer is:

$$\sigma_v = -J\frac{1}{T_p}(\mu_T^g - \mu_T^p) \tag{14}$$

With the ideal gas assumption the chemical potential difference for water from the moist sheet to the adjacent water vapor is:

$$\Delta\mu_T = \mu_T^g - \mu_T^p = RT_p \ln\frac{p^*}{p_p^*} \tag{15}$$

where p_p^* is the vapor pressure of the water in the moist sheet at the values of T_p and w at the sheet surface obtained from the dryer simulator, and p^* is the vapor pressure in the adjacent air. For Case 2 boundary conditions these equations apply with an area equal to the two sides of the sheet.

For Case 1 boundary conditions it is necessary to distinguish between the two sides of the paper. On the cylinder contact side of the sheet there can be no water vapor transport so here the entropy production rate, σ_c, is due to heat transfer alone:

$$\sigma_c = J'_{q,c}\left(\frac{1}{T_p} - \frac{1}{T_c}\right) \tag{16}$$

with $J'_{q,c}$ the heat flux from the cylinder to the paper and T_c the temperature of the cylinder surface. At the vapor transport side of the sheet while on the cylinder, the entropy production is due to both heat and mass transfer. The corresponding expression is the same as for Case 2 boundary conditions given in Eq. (13), but now with an area of transfer that is half that for Case 2.

The above expressions are now used to calculate the contributions to the total entropy production during drying. It is convenient to separate the entropy production between the contribution while the sheet is in contact with the cylinder, Eq. (16), and that when the sheet is passing through the dryer pocket between cylinders, the two terms in Eq. (10). The entropy produced when the sheet is in contact with the drying cylinders is:

$$\Delta\Sigma_c = \sigma_c\frac{\Delta t}{B} \tag{17}$$

This equation has been divided by B, the mass of dry paper per unit area (kg/m^2), in order to have the entropy production per kg of paper J/(kg K). Summing over all cylinders provides the total specific entropy production for cylinder heating. The corresponding contributions to specific entropy production from the heat flux and force, Eq. (13), and the mass flux and force, Eq. (14), are respectively:

$$\Delta\Sigma_a = \sigma_a\frac{\Delta t}{B} \tag{18}$$

$$\Delta\Sigma_v = \sigma_v\frac{\Delta t}{B} \tag{19}$$

These expressions apply to the transfer area provided by one cylinder. Summing over all cylinders provides the total specific entropy production per kg dry paper due to heat transfer between the sheet and the air, and due to the evap-

oration of water. It will subsequently be seen that the first of these terms is small relative to the second. The equations in this section also demonstrate the combined effect of several factors controlling the rate of entropy production. Therefore it is not possible to follow the effect from only one parameter, such as sheet temperature, when other factors such as cylinder surface temperature or ambient temperature are involved.

4. Methodology

4.1. Data inputs and calculations

Data are used for two grades of paper, linerboard and newsprint, produced on five paper machines. These machines all use steam heated cylinder conduction drying. Table 1 lists the main characteristics of the paper machines for which the entropy production analysis was applied. Each paper machine is identified with a code, LB for linerboard, NP for newsprint. For the linerboard machines the identification code indicates the basis weight of the product. The number of cylinders for each steam section and the corresponding steam pressures are recorded. Within each such steam section the condensing steam pressure can be assumed constant. Complete information on dryer surveys for these five cases is available [14,15].

The dryer simulator [14] has been used to provide the following performance parameters required for the present study: (i) local heat flux from the cylinder to the paper, (ii) local heat flux between the paper and the ambient air, (iii) surface temperature of each cylinder as well as sheet surface and average temperature, (iv) sheet surface and average moisture content, (v) water vapor flux from the paper for both types of boundary conditions. These data came in a time stream of values. The fluxes obtained from the simulator were used without modification. The thermodynamic forces of heat conduction required for entropy production calculations were obtained according to Eqs. (13) and (16). In order to calculate the thermodynamic driving force for evaporation, Eq. (15), the expression used for vapor pressure of moist paper was:

$$p_{\mathrm{p}}^{*} = \Theta(w, T_{\mathrm{p}})p^{*} \tag{20}$$

where p_{p}^{*} is the equilibrium vapor pressure at sheet surface T_{p} and w. For the sorption isotherm of moist paper, $\Theta(w,T_{\mathrm{p}})$, an empirical relation [14] based on the extensive desorption data from Prahl [19] was used:

$$\Theta(w, T_{\mathrm{p}}) = \exp(\beta_1 T_{\mathrm{p}} - \beta_2) \tag{21}$$

with

$$\begin{aligned} \beta_1 &= \exp(-15.03w - 1.37\sqrt{w} - 3.41) \\ \beta_2 &= \exp(-13.53w - 2.90\sqrt{w} + 2.90) \end{aligned} \tag{22}$$

According to Prahl [19] the sorption isotherms for paper made from various types of pulp are not significantly different. For vapor pressure of water, the correlation used in [14] was:

$$p^{*}(T_{\mathrm{p}}) = 133.322 \exp\left(18.3036 - \frac{3816.44}{T_{\mathrm{p}} - 46.13}\right) \tag{23}$$

The enthalpy of vaporization is derived from the above equilibrium vapor pressure correlation using the following expression derived from the Clausius–Clapeyron relation [19]:

$$\Delta_{\mathrm{vap}}H = -R\frac{\partial(\ln p^{*}/p^{0})}{\partial(1/T)} \tag{24}$$

with standard pressure p^{0}. Similarly, the sorption enthalpy is found from Eq. (21) with:

$$\Delta_{\mathrm{sor}}H = -R\frac{\partial(\ln \Theta)}{\partial(1/T)} \tag{25}$$

4.2. Mass and energy balances

The internal consistency of the data was checked, as described in Section 2. The mass balance was checked using Eq. (5) with the moisture content data and the integrated evaporation flux data. As can be seen from that equation, if the values of mass flux are integrated over a time interval and plotted against the relevant values of sheet moisture content, the sheet basis weight can be computed from the slope of the resulting line. The line presented in Fig. 2 is for the 337 g/m^2 linerboard case, identified as LB337. The basis weight computed this way could then be compared to the actual sheet basis weight as a measure of data consistency. Such calculations, performed for all cases, demonstrated that the average difference between the measured and calculated basis weight for the three linerboard

Table 1
Main characteristics of dryer sections used in this study

Paper machine	Grade	Basis weight (g/m^2)	Cylinder no.	Steam pressure (kPa gauge)	Speed (m/min)
LB183	Linerboard	183	1–11	335	378
			12–27	381	
			28–43	405	
			44–55	394	
LB205	Linerboard	205	1–11	573	391
			12–27	674	
			28–43	496	
			44–55	685	
LB337	Linerboard	337	1–18	600	374
			19–38	700	
			39–71	725	
			72–85	800	
NP1	Newsprint	48.8	1–16	13.8	542
			17–30	62.1	
			31–46	121	
NP2	Newsprint	48.1	1–16	69	539
			17–30	124	
			31–46	166	

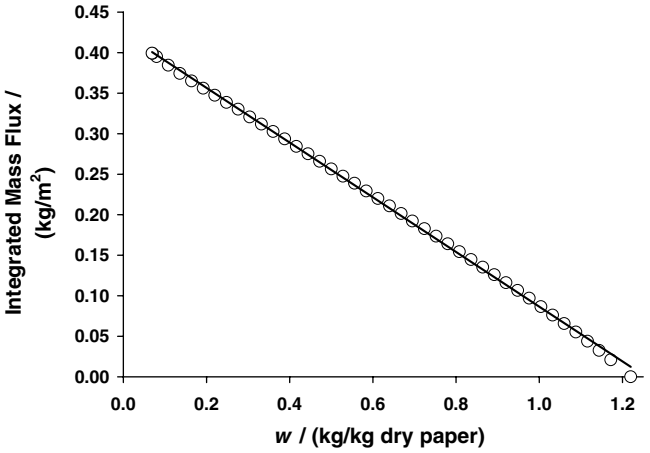

Fig. 2. Mass balance consistency check for the LB337 case. The regression line provides the basis weight according to Eq. (5).

cases was only 3% and that of the two newsprint cases was 10%, providing an acceptable consistency check.

Next the energy balance, Eq. (9), was used with Eq. (7) for the enthalpy of vaporization. The assumptions used for Eqs. (7)–(9) were noted earlier. The two contributions to the vaporization enthalpy were calculated, using Eq. (23) for bulk water vapor pressure, Eq. (21) for water desorption, and Eqs. (24) and (25). The desorption enthalpy contributed up to 10% of the enthalpy change, but the contribution was only significant towards the dry end of the paper machine, as is well known.

In Fig. 3 the integrated heat flux, the left-hand side of Eq. (9), is compared cylinder by cylinder with the right hand side, demonstrating acceptable agreement for the same case as used for Fig. 2. These values of Fig. 3 line are seen to overestimate those of Fig. 3 points, obtained from the right side of Eq. (9), over the intermediate part of the dryer section while providing an underestimate towards the end of the dryer section. In a system as complex as this, it is not possible to identify the sources of the differences seen in Fig. 3. One unavoidable source

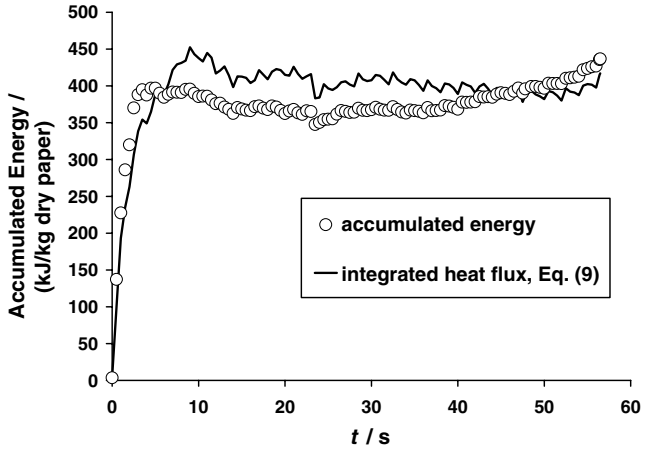

Fig. 3. Energy balance consistency check for the LB337 case from Eq. (9).

of these differences is that Eq. (9) assumes that there is a uniform sheet temperature and moisture content across the sheet thickness although the drying simulation work [10,12,14,15] has clearly established that there are frequently large differences in the thickness direction which are by no means linear with thickness. As the use of representative values in Eqs. (8), (9) and (20)–(25) introduces approximations into the procedure, it is reassuring that the final differences are as small as identified in Fig. 3.

5. Entropy production results

5.1. Three drying regimes

For the paper machine producing 337 g/m^2 linerboard, identified as LB337, Fig. 4 presents the development over its 85 cylinders of the three contributions to entropy production per kg dry paper from Eqs. (17)–(19). The contributions $\Delta\Sigma_c$, $\Delta\Sigma_v$ and $\Delta\Sigma_a$ are due, respectively, to cylinder conduction, evaporation and paper-ambient convection. Fig. 4 shows the discontinuities which occur at the boundaries of the four sections of cylinders because of the changes in steam pressure between sections, as recorded in Table 1. Not only are there step changes in cylinder temperature at the boundaries between the sections, but in addition the length of sheet from one cylinder to the next is different at the three break points between the sections. These various effects give rise to the discontinuities between cylinders 18–19, 38–39 and 71–72 in Fig. 4. The contributions to specific entropy production from evaporation and from cylinder heat transfer are generally of comparable magnitude, while that from the heat transfer between the sheet and ambient is negligible by comparison. The low level of entropy production by the latter term, i.e. by sheet-ambient air interaction, is not a general characteristic but applies for the specific LB337 machine. In the present case this term is relatively low for two reasons: this paper machine used an ineffective dryer pocket air ventilation system, providing only low temperature air, and the basis weight is very high, at 337 g/m^2. With a high flow rate of hot, relatively dry pocket air, this term would be higher. As an example for effective pocket ventilation, the pocket air temperature without the injection of hot air could be around 40 °C while the injected air temperature could be as high as 120 °C. Likewise, for lower basis weight sheets this effect relative to other two terms would be proportionally higher.

Three drying regimes can be identified, and these do not coincide with the steam pressure sections of the dryer. The first drying period occurs over cylinders 1–10, where entropy production from heating the sheet starts at a very high level and decreases steadily, cylinder by cylinder, to approach the average level at about cylinder 10, which marks the end of this drying regime. Correspondingly, in this drying regime the entropy produced by evaporation of water rises from zero to reach, by cylinder 10, about

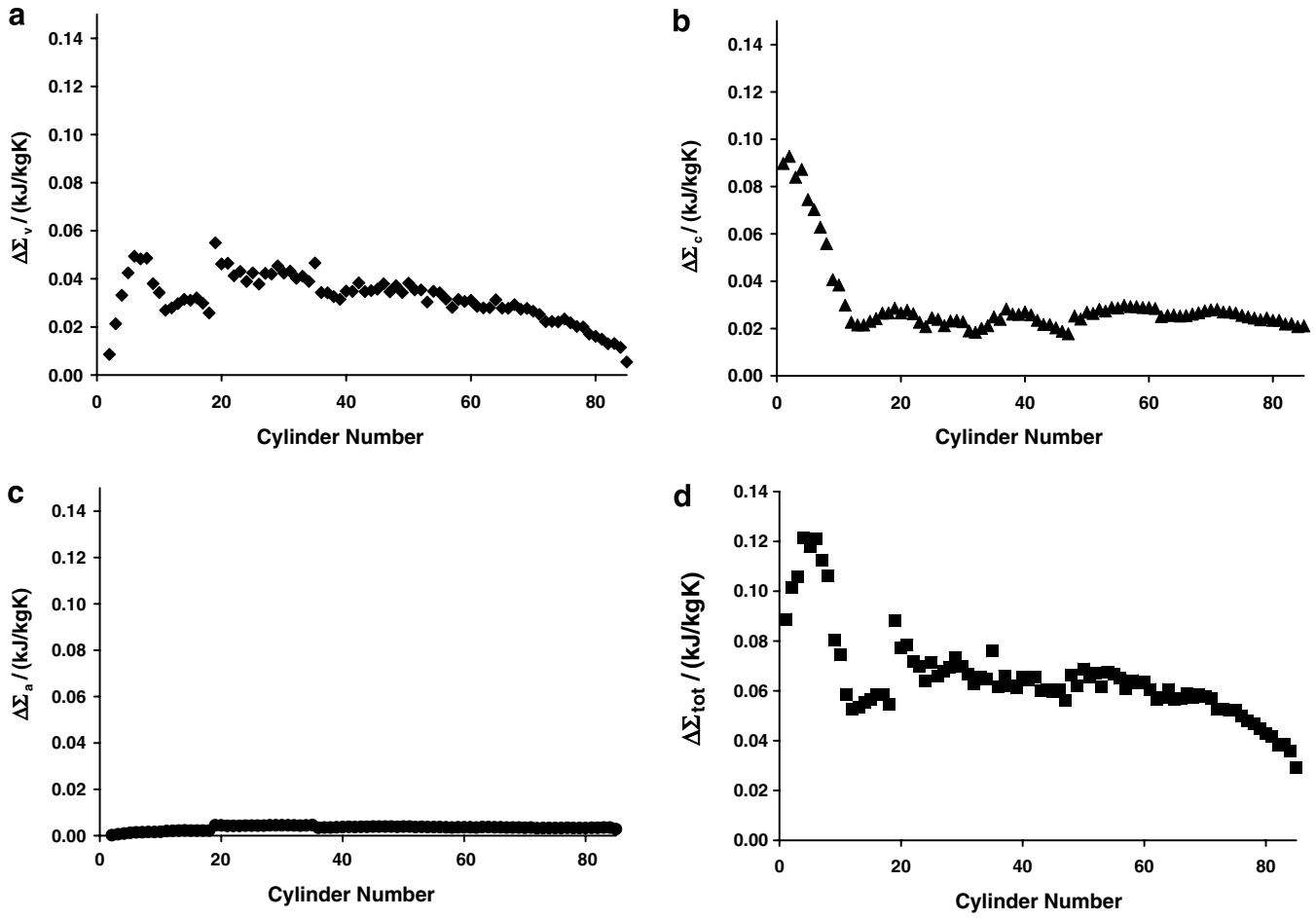

Fig. 4. Entropy components and total entropy production per kg dry paper for the LB337 case: (a) evaporation contribution, (b) heat conduction contribution, (c) heat convection contribution, (d) total entropy production.

the average level for the rest of the dryer. By the end of the first drying regime the entropy produced by cylinder heating and by evaporation are comparable. During the second drying regime, over about cylinders 10–53, all contributions to entropy production are relatively steady. In the third drying regime, from about cylinders 53–85, the entropy produced by cylinder heating remains stationary while that from evaporation decreases to a low value.

Fig. 5 presents the sheet moisture content, cylinder by cylinder, as determined by the dryer simulator [14,15] at the sheet surface, sheet centerline and thickness direction average. Fig. 5 shows that for much of the dryer, large moisture gradients develop across the sheet thickness, producing conditions with a region near the sheet surface where the pores are empty of free water and with some bound water in the fibers at moisture content below 0.2 kg/kg dry paper, while the interior of the sheet may have saturated fibers and abundant free water in the pores. The first drying regime corresponds to the warm-up period which is the period of increasing drying rate where most of the heat added appears as sensible heat, increasing the sheet temperature substantially. This well-recognized period of increasing drying rate is seen on Fig. 4 to correspond to that for increasing entropy production. It is now seen

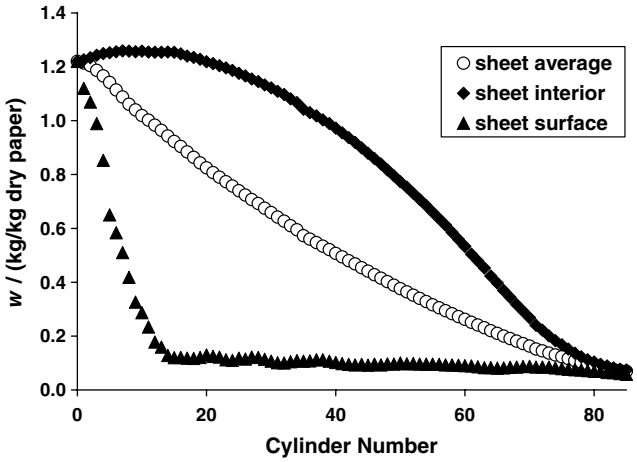

Fig. 5. Moisture content profiles for the LB337 case.

from Fig. 5 that this regime ends when, at the sheet surfaces, the free water has been removed from the interfiber pores and the fiber walls.

Between cylinders 10 and 53, Fig. 5 shows that over the sheet thickness the local conditions range from fairly dry fibers at its surfaces, to saturated fibers at its centerline with

free water in the pores at moisture contents above that of the fiber saturation point (FSP), about 0.7 kg/kg dry paper for this grade of paper. This pore water is transported by capillary action towards the surface, evaporates, and leaves as water vapor. In this period, commonly designated the period of constant drying rate, the evaporation rate is roughly constant, with the rate of water supplied from the interior being roughly constant. Fig. 5 shows that the second drying regime ends, at about cylinder 53, when the moisture content at the middle of the sheet has decreased to the FSP, thus ending the ready supply of water to the sheet surfaces.

Over the cylinders 53–85 sector towards the dry end of the paper machine, the period of falling drying rate corresponds to the third entropy regime, that of decreasing entropy production as seen in Fig. 4. Here the drying rate decreases because there is no free water remaining in the interfiber pores to provide rapid capillary transport of moisture to the sheet surface where heat is received from the hot drying cylinder surfaces. In this drying region, the water in the fiber walls is being removed [20–22]. At about cylinder 53 it is seen from Fig. 4 that the total entropy production, $\Delta\Sigma_{tot}$, ends its approximately constant period and starts a steady decrease towards the end of the dryer section. The average paper temperature rises in this third drying regime. The specific entropy production from evaporation is seen from Fig. 4 to decrease substantially during this regime, although that for heat conduction from the cylinder decreases only moderately. This combination of effects results from the increasing enthalpy of evaporation of the remaining water as it is increasingly strongly sorbed to the fibers. Below a moisture content of about 0.15 kg/kg dry paper the sorption enthalpy of the water on the fibers, determined by Eqs. (21) and (25), starts to become significant, i.e. more than 10% of the bulk water value.

Although the detailed results, cylinder by cylinder, are shown in Fig. 4 only for the case of the 337 g/m^2 linerboard machine, the same three drying regimes according to entropy production are distinguishable also for the other 4 dryer sections tested.

5.2. Entropy production and drying process operations

The entropy production components per kg dry paper for the 5 paper machines are compared in Table 2. Unlike the values of Fig. 4, which represent the contributions to entropy prediction for individual cylinders, Table 2 records the total entropy production for the entire dryer section of each paper machine. It is a characteristic common to these 5 paper machines that the entropy production for evaporation and for heat conduction to the sheet are of the same order of magnitude while the contribution due to convection heat transfer between the sheet and the ambient air is of minor importance. As noted earlier, this last characteristic would not apply for machines with efficient dryer pocket ventilation systems.

Table 2
Total entropy production per kg dry paper, its components and the lost work assuming an environmental temperature of 300 K

Paper machine	Evaporation (kJ/kg K)	Conduction (kJ/kg K)	Convection (kJ/kg K)	Total (kJ/kg K)	Lost work (kJ/kg)
LB183	0.75	0.90	0.04	1.69	507
LB205	0.79	0.90	0.01	1.69	507
LB337	0.94	1.20	0.11	2.26	678
NP1	0.37	0.59	0.10	1.06	318
NP2	0.58	0.81	0.03	1.42	426

In order to compare the total entropy production values for the 5 machines we include, in Table 2, the lost work per kg dry paper, which is derived from the Gouy–Stodola equation (1) using 300 K as environment temperature. These values can be compared with the energy requirement (the energy required to heat and evaporate water from 50 °C to 100 °C) given by de Beer et al. [2] who present the value of 2.63 MJ/kg dry paper for an ingoing sheet of 45% dry solids. The lost work values presented in Table 2 constitute less than 20% of this value. The exergy loss (lost work) in the dryer section was given by de Beer et al. as 1.9 MJ/kg dry paper, well above our values in Table 2. This difference might be due to the higher efficiency of dryer sections studied here, although de Beer et al. do not provide enough information to make a direct comparison possible.

The contributions to the total entropy production per kg dry paper listed in Table 2 derive from the intrinsic nature of the paper making process. For example, the results presented on Fig. 4 show that the highest entropy production occurs during the sheet warm-up period which starts at the wet end of dryer section. This contribution to total entropy production is unavoidable because the wet sheet reaches the dryer relatively cool and must be warmed before evaporation can start. Numerous other constraints also limit the type of changes that could be made to minimize entropy production. Thus dryer sections are typically divided into several steam subsections, in each of which the steam pressure inside the dryer cylinders is constant. There are several important product quality and operational reasons why the steam pressure in the cylinders must be increased from the wet end towards the dry end of the dryer. Thus the thermal driving force, which is the difference between the inverse of condensing steam temperature in the cylinder and the inverse of the temperature of moist sheet in contact with the cylinder, changes throughout the dryer.

Although process limitations such as the one described above might limit the type of changes favored by entropy production analysis, several studies on the second law optimization of process equipment have been reported [7,8,23]. Johannessen and Kjelstrup [23] used optimal control theory to minimize the entropy production in a plug flow reactor and showed that high energy efficiency could be achieved when driving forces for entropy production are kept con-

stant in particular sections of the reactor. They used the temperature of cooling/heating medium and the reactor length as control parameters and devised several scenarios which could reduce the entropy production by up to 25% while maintaining the production requirements. The concept of keeping the driving forces of entropy production constant could be applicable to paper drying. For example, while the condensing steam temperature throughout the cylinders is usually dictated by process considerations, the temperature and humidity of dryer pockets could be controlled by effective pocket ventilation as discussed before. Therefore it could be possible to devise scenarios, through adjusting the temperature of injected air to the pockets, which would result in constant entropy production over certain parts of dryer section and, consequently, higher energy efficiency. Such process optimization based on the results of the present study is the subject of future work.

There is considerable difference between the entropy production of the 5 dryer sections. For example, the total entropy production per kg dry paper for the NP2 case, Table 2, is 35% higher than that for NP1. These two cases are for the same paper machine at different times, for which the difference in paper basis weight is unimportant: 48.8 and 48.1 g/m^2. However from the NP1 to NP2 case there was an increase in the moisture content of the sheet entering the dryer section, from 1.53 to 1.63 kg/kg dry paper, and a corresponding increase in the amount of water removal per kg dry paper. Thus this difference in amount of water removed per kg dry paper has the natural consequence of contributing to the increase in specific entropy production per kg dry paper from 1.06 to 1.42 kJ/K kg paper, as seen in Table 2. Different grades of paper enter different dryer sections at widely varying moisture contents, over the approximate range of 1.2–1.7 kg water/kg dry solids, with variation also in moisture content of the sheet exiting the dryer section. It follows that normalizing entropy production per kg dry paper mixes the entropy production coming from different variables. Thus, expressed per kg dry paper, the entropy production from the irreversibilities in the processes of heat and mass transfer detailed in Section 3 includes the entropy production proportional to the amount of water removed per kg dry paper. To clarify the entropy analysis the latter effect on entropy production should be allowed for. This may be achieved by normalizing entropy production to "kg water removed" rather than to "kg dry paper". This alternative basis of normalization is done by division of the Table 2 values, expressed per "kg dry paper", by the ratio "kg water removed/kg dry paper". The latter quantity is known precisely for any paper machine, being the difference between the dry basis moisture contents entering and leaving the dryer section, w_{in}–w_{out}. Table 3 provides the two bases for total entropy production.

Table 3
Alternative normalization of specific entropy production of paper dryers

Paper machine	$w_{in} - w_{out}\left(\frac{\text{kg water removed}}{\text{kg dry paper}}\right)$	Specific entropy production (kJ/kg K)	
		Per kg dry paper	Per kg water removed
LB183	1.16	1.69	1.46
LB205	1.16	1.69	1.46
LB337	1.15	2.26	1.97
NP1	1.45	1.06	0.73
NP2	1.55	1.42	0.91

A more rational analysis may now be obtained for the total entropy production in the NP1 and NP2 dryer sections. With the specific entropy production normalized in these alternative ways, the NP2 machine shows an entropy production which, per kg dry paper, is higher by 35% but, per kg water removed, is higher by 25%. The 35% difference includes the entropy production associated with the removal in NP2 of significantly more water per kg dry paper.

With respect to the differences in heat and mass transport process irreversibilities, it should be noted it was necessary that, from the NP1 to the NP2 case, the paper production rate be reduced as little as possible in spite of the increase in evaporation load on the dryer section. Consequently the condensing steam pressure in the cylinders was increased for the NP2 case. Thus as recorded in Table 1 the steam pressures of the NP1 case, 13.8, 62.1 and 121 kPa, were increased significantly for the NP2 case to 69, 124 and 166 kPa (gauge pressure values). These increases in steam pressure produce corresponding increases in cylinder surface temperature, hence higher thermal driving forces throughout the dryer section and thereby higher entropy production for NP2 than NP1. Thus the higher specific entropy production for the NP2 operating conditions is an unavoidable consequence of techno-economic constraints on the industrial operation. These results illustrate the impact of choice of operating conditions on the total entropy production.

Analysis of the three cases for linerboard production provides another perspective on factors related to entropy production. The values of condensing steam pressures for these three cases, detailed in Table 1, show that higher steam pressures were used for the LB337 case which, as discussed above, would lead to higher entropy production. There are also large differences in basis weight, covering the range 183–337 g/m^2. The sheet thickness covers a correspondingly wide range, from 258 to 475 microns for the dry sheet. The heat and mass transfer resistance to drying increases with sheet thickness. Thus there is an increase in the resistance for heat conduction from the heated cylinder surfaces into the interior of the sheet where analysis shows that all evaporation occurs [14]. With increasing sheet thickness there is likewise an increase in the resistance for mass transfer of the water vapor from the interior of the sheet to the vapor transport side. With increasing basis weight there is then an increase in the resistance to the basic transport processes of drying. The dynamics of

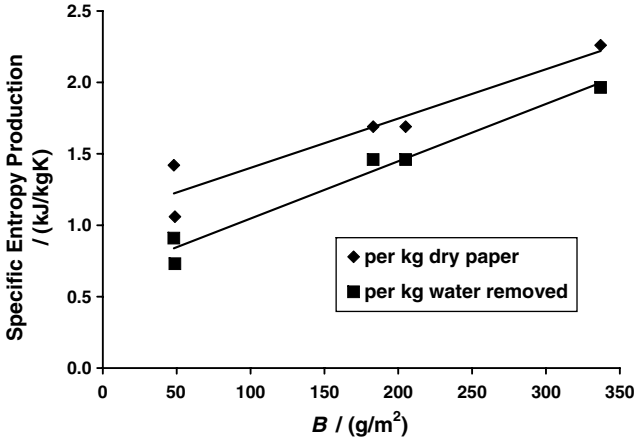

Fig. 6. Effect of paper basis weight on specific entropy production.

transport phenomena inside the sheet are reflected in the entropy production calculation. In contrast to the case of NP1 and NP2 where the differences included a significant increase in the amount of water removed per kg dry paper, for the three linerboard machines there is no significant difference in this respect, the water evaporated being in the range 1.15–1.16 kg/kg dry paper for the three machines. With this aspect being the same, the specific entropy production for the 337 g/m^2 sheet is 34% higher whether it is normalized to kg dry paper or kg water removed.

These perspectives for the three linerboard and two newsprint machines are summarized in Fig. 6 with the specific entropy production displayed with both alternate bases of normalization. It is apparent that there is less scatter of the results when specific entropy production is normalized to "kg water removed", as this basis removes the source of difference in entropy production due to difference in the amount of water removed per kg dry paper. Thus, the R^2 correlation value for the results in Fig. 6 is 0.91 for normalization to kg dry paper, 0.97 for entropy production relative to kg water removed.

Even with specific entropy production normalized to the amount of water removed, paper basis weight on Fig. 6 is of course not the only factor relevant to entropy production. For the NP1 to NP2 cases of the same basis weight the above analysis noted the increase in entropy production with the increased irreversibility from use of higher cylinder surface temperatures. However when the entropy production is normalized to allow for the higher water removal from newsprint, the specific entropy production for newsprint averages about 0.8 kJ/K kg while that for the linerboard grades averages about 1.6 kJ/K kg water removed. Thus the irreversibilities associated with heat and mass transfer across moist paper during drying are reflected in the high sensitivity of specific entropy production to basis weight that is apparent in Table 3 and Fig. 6 representation of results.

6. Conclusions

For the process of drying paper by the cylinder drying technique the present study presents the first analysis based on irreversible thermodynamics, with linerboard and newsprint used as specific examples. The variation in the entropy production from the inlet to the exit of the dryer permits identification of three entropy production regimes for drying, which have been related to the recognized periods of increasing, constant and falling drying rate. This approach extends the process engineering modeling of the drying of webs [24]. The procedure developed here for entropy production analysis could be used as a benchmarking tool, providing a quantitative measure for the energy efficiency of a dryer section and to assist mills in improving energy efficiency.

The total entropy production for a paper dryer derives from irreversibilities in the transport processes involved in drying. The magnitude of these irreversibilities depends in turn on the characteristics of the sheet and on the design and operating conditions of the dryer. Of the numerous sheet characteristics the present study enabled determination of effect of paper basis weight on specific entropy production. Of dryer operating characteristics the test data used showed the sensitivity of specific entropy production to condensing steam pressure in the dryer cylinders.

When the specific entropy production is normalized per kg water removed rather than per kg dry paper, the effect on entropy production coming from the variation in moisture content into and from paper dryer is allowed for, enabling clear identification of the sensitivity of specific entropy production to sheet and dryer characteristics. However both bases of normalizing entropy production have their role. In this process, dry solids into the dryer = dry solids out, so that what the process accomplishes is "kg water removed per kg dry solids". Specific entropy production per kg water removed thereby provides the more scientific basis, one which relates more directly to the process. However as the objective of a paper mill is to produce dry paper, specific entropy production per kg dry solids relates to the overall objective of the process. Thus depending on the focus of interest, either of the bases presented here for specific entropy production may be employed.

Although cylinder drying is currently the dominant process in the production of printing and heavier grades, there is gradual recognition in the paper industry that better drying techniques with higher capacity are needed in the future. An attractive alternative is the combination of conductive cylinder drying with convective impingement drying, the latter already in use for tissue and toweling, thereby producing hybrid dryer sections for printing and heavier grades. The present work has therefore the potential to be used as a tool not only for assessing the efficiency of existing dryer sections but also to evaluate new drying technologies and to provide an additional technical basis for the current debate on the choice for dryer technology of the future.

Acknowledgements

G. Koper thanks the Norwegian Research Council for a research grant making it possible to dedicate his sabbatical leave to this work. M. Sadeghi is grateful to the same source for a travel bursary. The authors thank A. Zvolinschi for useful discussions.

References

[1] Energy Efficiency Improvement Utilizing High Technology, World Energy Council, London, 1995.
[2] J. de Beer, E. Worrel, K. Blok, Long-term energy-efficiency improvements in the paper and board industry, Energy 23 (1998) 21–42.
[3] J. Manninen, T. Puumalainen, R. Talja, H. Pettersson, Energy aspects in paper mills utilizing future technology, Appl. Therm. Energy 22 (2002) 929–937.
[4] S. Kjelstrup, D. Bedeaux, Elements of Irreversible Thermodynamics for Engineers, International Centre of Applied Thermodynamics, Istanbul, 2001.
[5] Z. Kirova-Yordanova, Exergy analysis of industrial ammonia synthesis, in G. Tsatsaronis, M.J. Moran, F. Cziesla, T. Bruckner (Eds.), Proceedings of ECOS 2002, vol. III, Berlin, Germany, 2002, pp. 1369–1387.
[6] A. Bejan, Entropy Generation Minimization. The Method of Thermodynamic Optimization of Finite-Size Systems and Finite-Time Processes, CRC Press, New York, 1996.
[7] E. Johannessen, L. Nummedal, S. Kjelstrup, Minimizing the entropy production in heat exchange, Int. J. Heat Mass Transfer 45 (13) (2002) 2649–2654.
[8] L. Nummedal, M. Costea, S. Kjelstrup, Minimizing the entropy production rate of an exothermic reactor with constant heat transfer coefficient: The ammonia reactor, Indus. Eng. Chem. Res. 42 (2003) 1044–1056.
[9] S.R. de Groot, P. Mazur, Non-Equilibrium Thermodynamics, Dover, London, 1984.
[10] J.-F. Bond, V.G. Gomes, W.J.M. Douglas, Computer simulation of drying paper by multiple techniques, Pulp Paper Canada 97 (1996) T433–T435.
[11] G. Fralic, G. Glendenning, D. Guertin, R.B. Kerr, J.-F. Bond, W.J.M. Douglas, Computer aided engineering of paper machine dryer sections, in: Proceedings of 1997 TAPPI Engineering Conference, Nashville, TN, 1997, pp. 143–149.
[12] S. Sidwall, J.-F. Bond, W.J.M. Douglas, Industrial validation of a multiple technique paper drying simulator, in: Proceedings of 1999 TAPPI Engineering Conference, Anaheim, CA, 1999, pp. 271–301.
[13] S. Sidwall, M. Sadeghi, W.J.M. Douglas, Comparative structures for simulation of paper drying, in: Proceedings of 1999 TAPPI Engineering Conference, Anaheim, CA, 1999, pp. 239–270.
[14] M. Sadeghi, Modeling and simulation of transport phenomena in paper drying, PhD thesis, McGill University, Montreal, Canada, 2003.
[15] M. Sadeghi, W.J.M. Douglas, From tissue to linerboard: validation of a microscale simulator for single technique and hybrid dryers, in: Proceedings of the 14th International Drying Symposium, vol. A, Sao Paulo, Brazil, 2004, pp. 444–451.
[16] S.J. Hashemi, V.G. Gomes, R.H. Crotogino, W.J.M. Douglas, In-plane diffusivity of moisture in paper, Drying Technol 15 (1997) 265–294.
[17] D. Bedeaux, S. Kjelstrup, Transfer coefficients for evaporation, Physica A 270 (1999) 413–426.
[18] A. Rosjorde, D.W. Fossmo, D. Bedeaux, S. Kjelstrup, B. Hafskjold, Nonequilibrium molecular dynamics simulations of steady-state heat and mass transport in condensation. I. Local equilibrium, J Coll Interf Sci 232 (2000) 178–185.
[19] J.M. Prahl, Thermodynamics of paper fiber and water mixtures, PhD Thesis, Harvard University, Cambridge, MA, 1968.
[20] L. Tie-Qiang, U. Henrikson, L. Odberg, Deformation of pores sizes in wood cellulose fibers by 2 H and 1H NMR, Nordic Pulp Paper Res. J. 8 (1993) 326.
[21] B. Alince, T.G.M. van de Ven, The Fundamentals of Papermaking Materials, in: Transactions of 11th FRC, vol. 2, Cambridge, UK, 1997 (Chapter: Porosity of swollen fibers evaluated by polymer adsorption).
[22] C.H. Hunt, R.L. Blaire, J.W. Rowen, Submicroscopic structure of cellulose from nitrogen sorption measurements, Textile Res. J. 20 (1950) 43.
[23] E. Johannessen, S. Kjelstrup, Minimum entropy production rate in plug flow reactors: An optimal control problem solved for SO_2 oxidation, Energy 29 (2004) 2403–2423.
[24] M.J. Lampinen, K.T. Ojala, Advances in Transport Processes, vol. IX, Elsevier Science Publishers B.V., 1993 (Chapter: Mathematical modeling of web drying).